SHEATH PROPERTIES AND RELATED PHENOMENA OF THE PLASMA WALL INTERACTION IN MAGNETISED PLASMAS. APPLICATION TO ITER

V. Anita, C. Agheorghiesei, S. Costea, C. Costin, G. Popa, L. Sirghi, M. L. Solomon

Alexandru Ioan Cuza University, Iasi

1. Overview

The research directions followed this year are in accordance with two major areas of EFDA interest, namely *Plasma diagnostics* and *Theory and modelling*. Plasma diagnostics experiments were performed on Pilot-PSI, a linear magnetized plasma device at FOM Institute for Plasma Physics "Rijnhuizen", The Netherlands, Association EURATOM/FOM. Two types of electrostatic probes were used to characterize the plasma: (*i*) Katsumata probe for measuring the cross-field diffusion coefficient and (*ii*) a multi-channel analyzer for measuring the time-space distribution of plasma current and floating potential in front of the target. The measurements of the diffusion coefficient were achieved in collaboration with researchers from the Institute for Ion Physics and Applied Physics, University of Innsbruck, Association EURATOM-ÖAW, Austria. The modelling research was focused on the development of numerical codes for the simulation of magnetised plasma devices with application to Pilot-PSI. Two bi-dimensional (*r*,*z*) codes, based on fluid and Particle-In-Cell approach, were envisaged.

Publications

[1] M. L. Solomon, I. Mihaila, V. Anita, C. Costin, G. Popa, H. Van der Meiden, R. S. Al, G. Van Rooij, N. L. Cardozo, J. Rapp, C. Ionita, R. Starz, R. Schrittwieser, "Measurements of plasma diffusion coefficient in Pilot-PSI device using Katsumata probe", *Inter-Academia 2009*, Warsaw, Poland, 14-17 September 2009, published in *Journal of Automation, Mobile Robotics and Intelligent Systems* **3**(4), 160-163 (2009)

[2] M. L. Solomon, I. Mihaila, V. Anita, C. Costin, G. Popa, H. J. van der Meiden, R. S. Al, M. J. van de Pol, G. J. van Rooij, N. J. Lopes-Cardozo, J. Rapp, "Multi-channel analyzer investigations of ion flux at the target surface in Pilot-PSI", *8th International Workshop on Electric Probes in Magnetized Plasmas*, Innsbruck, Austria, 21-24 September 2009

2. Characterisation of Pilot-PSI plasma beam by electrical methods (different types of probes, electrostatic analysers, etc)

One of the main research topics on Pilot-PSI concerns the interaction of magnetized plasma with a solid surface in extreme conditions (of particle and energy fluxes), typical for the divertor of a fusion reactor. Our mission in the collaboration with FOM Institute is to develop and use different electrical methods based on probes and electrostatic analyzers to characterize the plasma beam generated by the source of Pilot-PSI device.

2.1. Katsumata probe measurements for the radial diffusion coefficient

The Katsumata probe was inserted in the vacuum chamber at 3.4 cm in front of the target, with its axis perpendicular to the magnetic field lines. The fluctuations of the floating potential were measured at different radial positions of the probe (*R*) and also for different depths of the collector inside the ceramic tube (*h*). The radial position ranged between 0 and 2 cm, referenced

to the axis of the vacuum vessel. The collector was retracted inside the ceramic tube at a maximum depth of 5 mm. The method used to process the data for a Katsumata probe is the one described by J. Brotankova *et al* in reference [1].

The spectra of signal fluctuations are shown in figure 1 for a radial position of the Katsumata probe R = 0.4 cm and depths of the collector inside the ceramic tube h = 0÷5 mm. It can be noticed that, as the collector is retracted inside the ceramic tube, the signal amplitude (A) decreases. The dependence of ln(A) on h is plotted in figure 2 for several frequencies (in the range of hundreds of KHz).

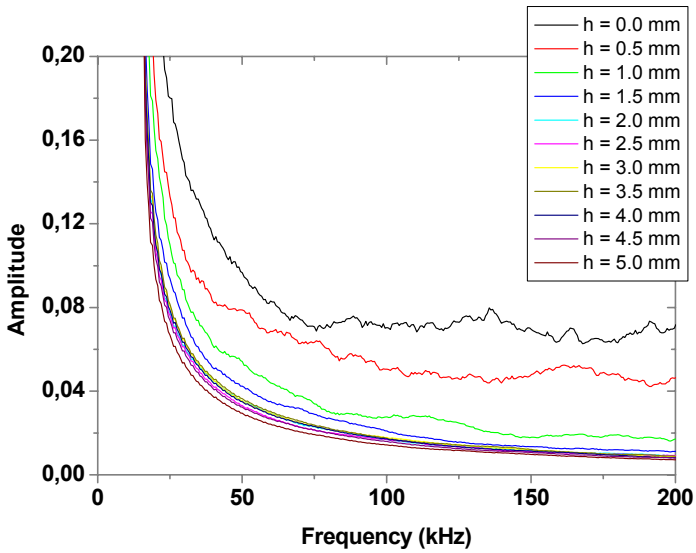

Figure 1: Amplitude spectra of the fluctuations on the probe's collector for different h positions

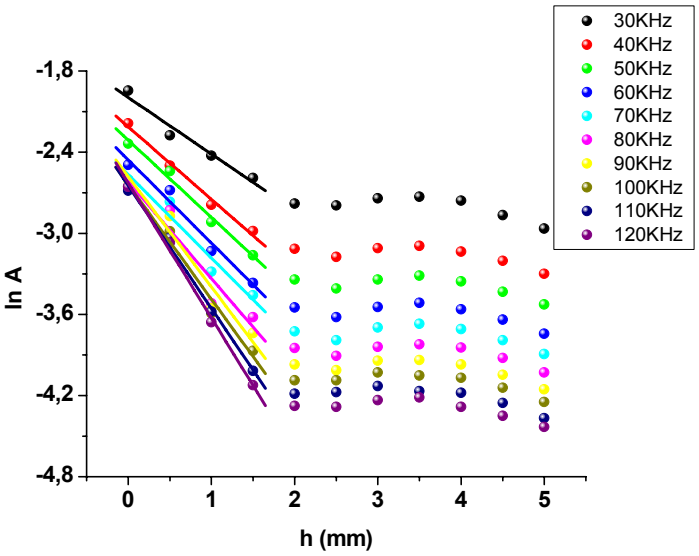

Figure 2: Decay of signal amplitude inside the ceramic tube

For h values smaller than 2 mm the amplitude logarithm decreases linearly, meaning that the amplitude signal registered by the Katsumata probe collector has an exponential decay. This behaviour is specific to a diffusion process of the plasma inside the ceramic tube. The dependence of $1/L^2$ (L is the diffusion length) on the frequency f (figure 3) is almost linear, in agreement with the diffusion theory [1] that stipulates:

$$1/L^2 = \pi f/D,$$

where D is the diffusion coefficient of the plasma inside the ceramic tube, perpendicularly to the magnetic field line. Thus, the transversal diffusion coefficient can be determined from the graph's slope.

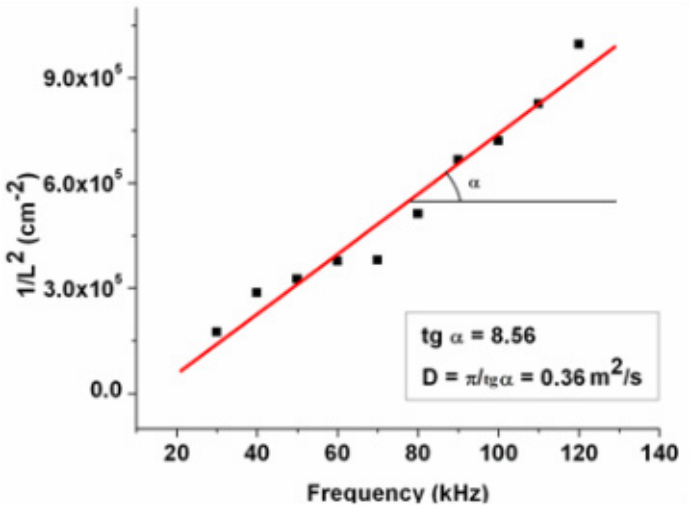

Figure 3: Dependence of $1/L^2$ on the frequency

For the measurements achieved in the experimental conditions of pressure p = 7.4 Pa, magnetic field B = 0.4 T, discharge current I_d = 90 A, gas flow Q_{H2} = 3 slm (standard litters per minutes), the obtained transversal diffusion coefficient slowly increased between 0.23 m^2/s in the centre of the plasma column (at the radial position R = 0 cm) and 0.74 m^2/s at the edge of the plasma column (at the radial position R = 1 cm). These values are in the same range as Bohm diffusion coefficient. For example, for an electron temperature of 1.7 eV measured on the axis of Pilot-PSI in a magnetic field of 0.4 T [2], the transversal Bohm diffusion coefficient is 0.27 m^2/s.

2.2. Multi-channel analyzer experiments

Milestone 1: *Current-voltage characteristics of the collectors*

The multi-channel analyzer with 61 collectors was placed in the centre of Pilot-PSI target. The first experiment consisted of drawing current-voltage characteristics of the collectors. Due to the complexity of the acquisition system required by all 61 collectors, these measurements were performed only on five collectors disposed at different radial positions (figures 4 and 5). Each collector has an identifying number (e.g. *ch 301*), the first figure of this number indicating the radial position of the collector: *0* indicates the centre of the analyzer, *1* → r = 2.5 mm, *2* → r = 5 mm, *3* → r = 7.5 mm and *4* → the outer radius, r = 10 mm. The discharge was operated in argon and hydrogen.

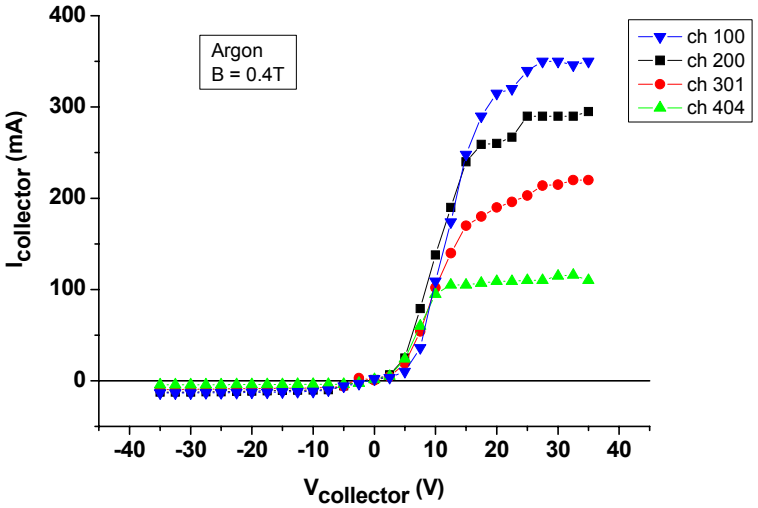

Figure 4: Collector current-voltage characteristics in Ar without carbon plate in front of the analyzer (B = 0.4 T, p = 4.5 Pa, I_d = 80 A, Q_{Ar} = 3 slm)

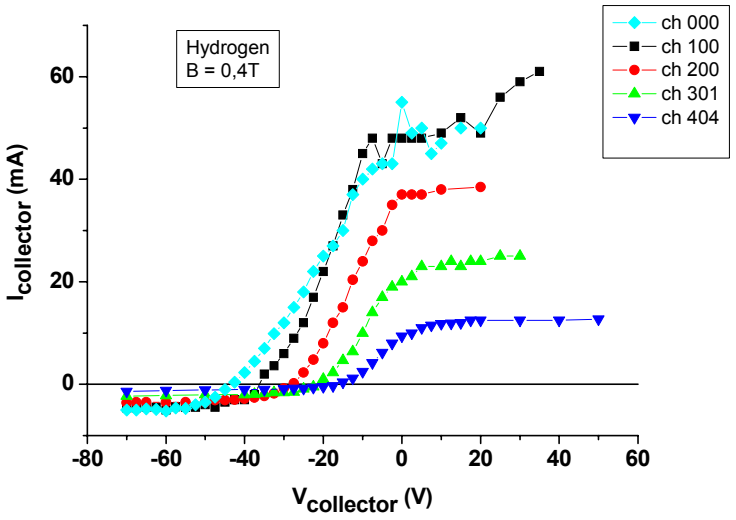

Figure 5: Collector current-voltage characteristics in H_2 without carbon plate in front of the analyzer (B = 0.4 T, p = 6.4 Pa, I_d = 100 A, Q_{H2} = 3 slm)

From both figure 4 and 5 one can extract the radial distribution of the saturation currents (electron and ion). While for argon (figure 4) the floating and plasma potential do not have a significant radial variation, in the case of hydrogen (figure 5) the radial variation of the two potentials is more than 20 V on 1 cm. Moreover, strong negative values of floating (-45 V) and "plasma potential" (-17 V) have to be noticed in the centre of the plasma column for hydrogen (*ch 000*). What is called here "plasma potential" is determined, according to Langmuir's theory as the probe voltage corresponding to the maximum of the first derivative of the I-V characteristic and it is as a rough approximation of the real plasma potential.

The I-V characteristics plotted in figures 4 and 5 are typical for "strong magnetized plasma", characterized by $a_{ce} < d_p < a_{ci}$, where $a_{ce,i}$ is electron and, respectively, ion Larmor radius and d_p is the characteristic dimension of the probe (probe radius). For the magnetic field of 0.4 T and typical temperature of the charged particles in Pilot-PSI of 1-4 eV [3], Larmor radii are a_{ce} ~ 10 μm, a_{cH} ~ 0.5 mm and a_{cAr} ~ 3 mm, while probe radius is 0.5 mm. In such "strong magnetized plasma" the ratio of the saturation currents I_{es}/I_{is} is much smaller than in the classical theory of the Langmuir probe. This theory predicts a ratio I_{es}/I_{is} of about 43 for hydrogen and 270 for argon discharge, but the present measurements show a ratio of only 10 for hydrogen and 20 for argon discharge. Stangeby developed a model [4] that explains this behaviour. So, for probe biased above the floating potential, electron flow to the probe is

constrained by momentum loss to the ions, generating two main effects: (*i*) an electron current increase slower than expected and (*ii*) an electron saturation current considerably diminished. In the same time the ion saturation current is about the same as in the classical theory.

As predicted by Stangeby, a large drop between floating and "plasma potential" appears in hydrogen due to the slower increase of the electron current, shifting the estimated "plasma potential" more positive than the real one. The higher plasma density is the slower electron current increases. Thus, a large difference is measured in hydrogen between the floating and "plasma potential" (~26 V) deduced from the current-voltage characteristic of the central collector *ch 000*. The larger radii of argon ions make the coupling between electrons and ions weaker in argon than in hydrogen discharge and, in the same time, reduce the radial inhomogeneity.

The ion flux to the target was estimated from the ion part of the current-voltage characteristic for each collector. At plasma densities up to 10^{20} m^{-3}, the measured ion fluxes are of 10^{22} - 10^{23} ions/m^2s (figure 6). A difference of a factor 4 was measured between the maximum ion flux in the centre of the target and the flux at the edge (1 cm radius) for hydrogen. It can be noticed that the plasma column is broader in argon than in hydrogen at the target surface.

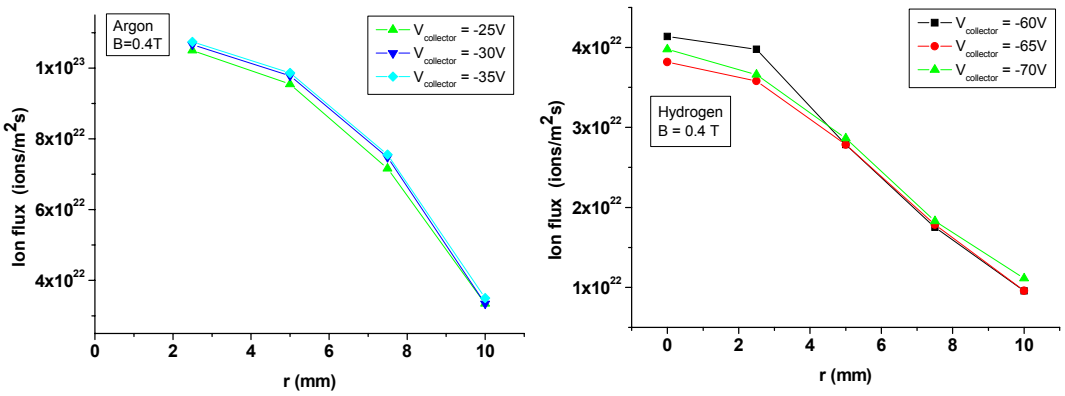

Figure 6: Radial profile of argon and hydrogen ion flux at the target surface

Milestone 2: *Spatio-temporal distributions of the floating potential and plasma current*

In the second experiment, all 61 collectors of the multi-channel analyzer were used in order to obtain information about the time-space distribution of plasma current and floating potential in front of the target. As in the case of the divertor, electrical diagnosis devices interact with dense plasma and the construction material must be high quality and temperature resistant. Our analyzer was made from machinable aluminum oxide ceramic (MACOR) with tungsten collectors and teflon coated wires. Optionally, a carbon plate can be added in front of the analyzer.

During the experiment it was noticed that copper is sputtered from the source due to the very high density plasma created inside. The sputtered copper deposits both on the target and the vessel's walls. As the multi-channel analyzer was placed in the centre of the target, its surface had to be regularly cleaned (daily). Moreover, previous experiments showed that the target is strongly heated during the plasma pulse. The maximum temperature obtained for tungsten or molybdenum targets is about 1600 K in the centre of the plasma column (the right side diagram in figure 7). Target heating was also evidenced in our experiments, the plasma beam affecting the analyzer surface. The surface made of MACOR was melted while tungsten collectors were not altered. This effect as well as copper deposition can be seen on the left side picture in figure 7.

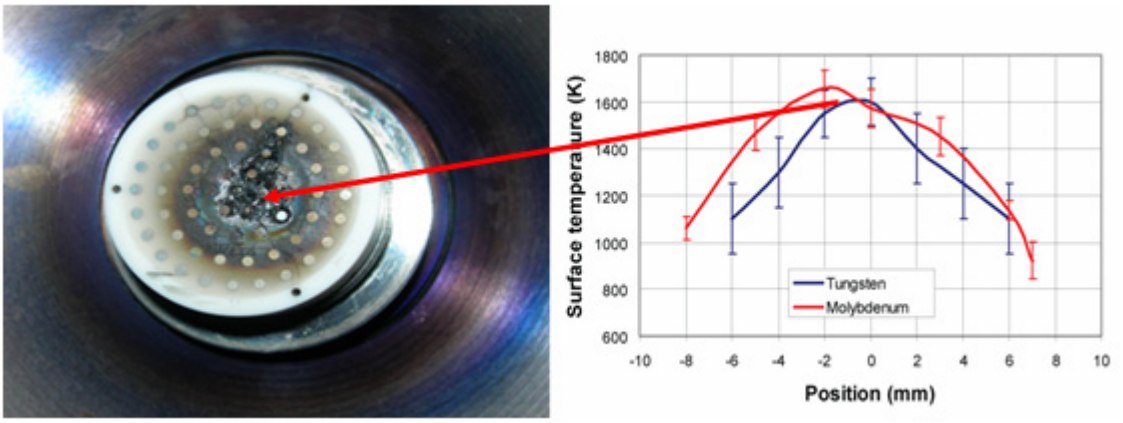

Figure 7: Analyzer surface after the interaction with the plasma beam

In order to register the current reaching the target, each collector was connected to the ground using a resistor of 0.2 Ω. The voltage drop on each resistor developed during ON-phase of the plasma (which is equivalent to the time interval when the magnetic field is applied) was registered by a high speed data acquisition system with maximum 64 inputs (National Instruments NI PXI 8106). Each measurement generates one digital file containing all 61 signals acquired from the analyzer's channels in time. The currents were registered for different magnetic fields (B = 0.4, 0.8 and 1.2 T) and different discharge currents flowing through the plasma source (I_d = 80, 100, 120 and 140 A).

Figure 8 shows the current variation measured during ON-phase of the plasma (shortly called 'pulse') on 9 collectors disposed along a diameter of analyzer. It reveals the big influence of the magnetic field intensity on currents distribution on the target. In the case of 0.4 T, current intensities are quite equal, with a maximum value of 0.8 A, and the plasma beam covers the entire surface of the analyzer (24 mm in diameter). By increasing the magnetic field to 0.8 T, the diameter of the plasma beam decreases, the plasma column is better confined in the centre of the chamber and the central collectors collect the highest current (9 A) while the current on the external collectors is approximately 4 A. It has to be mentioned that the signals plotted in all the figures have been smoothed using the adjacent averaging method by 150 points left and 150 points right. Nevertheless, the relative value of current fluctuations is still large at lower magnetic fields.

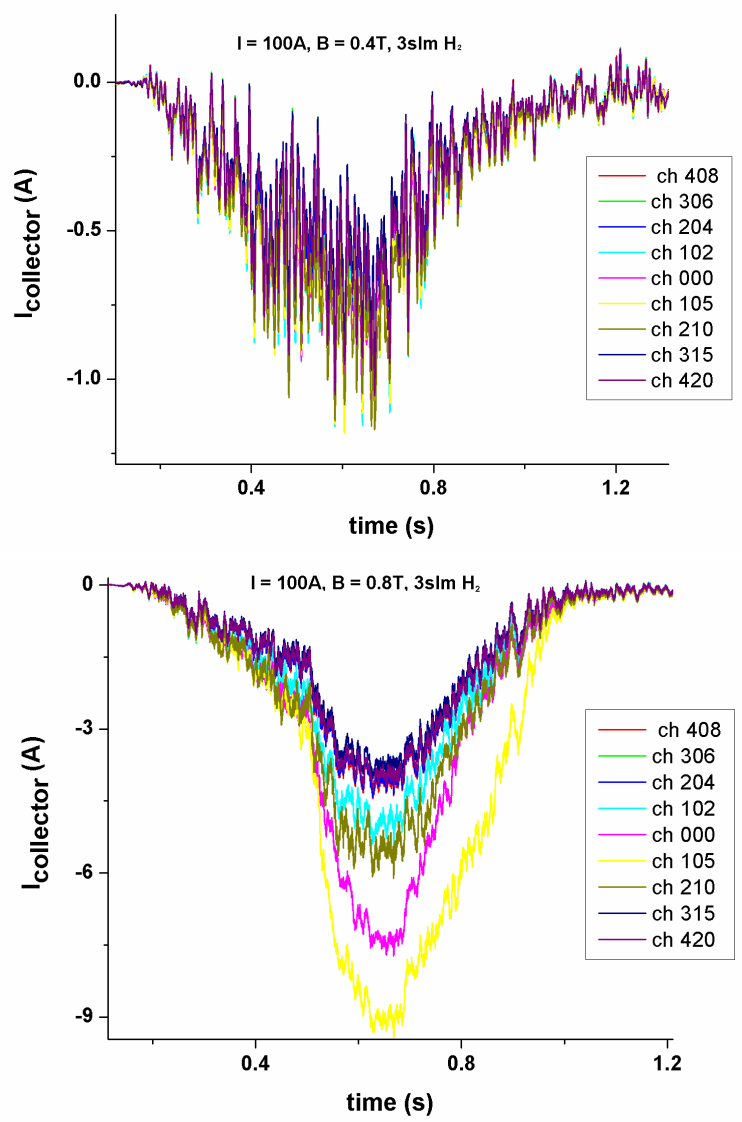

Figure 8: Current variation on 9 collectors during plasma pulse for B = 0.4 and 0.8 T (I_d = 100 A)

The radial distribution of the current reaching the target is plotted in figure 9 for two discharge currents, 80 and 100 A. The discharge current is concentrated mainly in the centre of the plasma beam. The increase of the discharge current from 80 to 100 A does not influence this distribution.

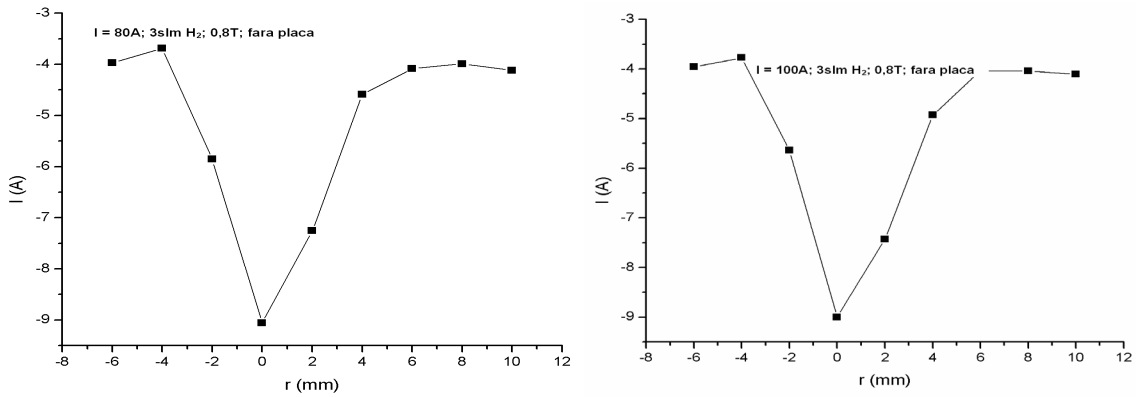

Figure 9: Radial distribution of the current at the target for I_d = 80 and 100 A (B = 0.8 T)

By using resistive dividers (10 MΩ and 10 kΩ) the floating potentials of the collectors were registered in different experimental conditions. Figure 10 shows the variation of floating

potentials during the plasma pulse for a discharge current of 80 and 100 A and a magnetic field of 0.4 T.

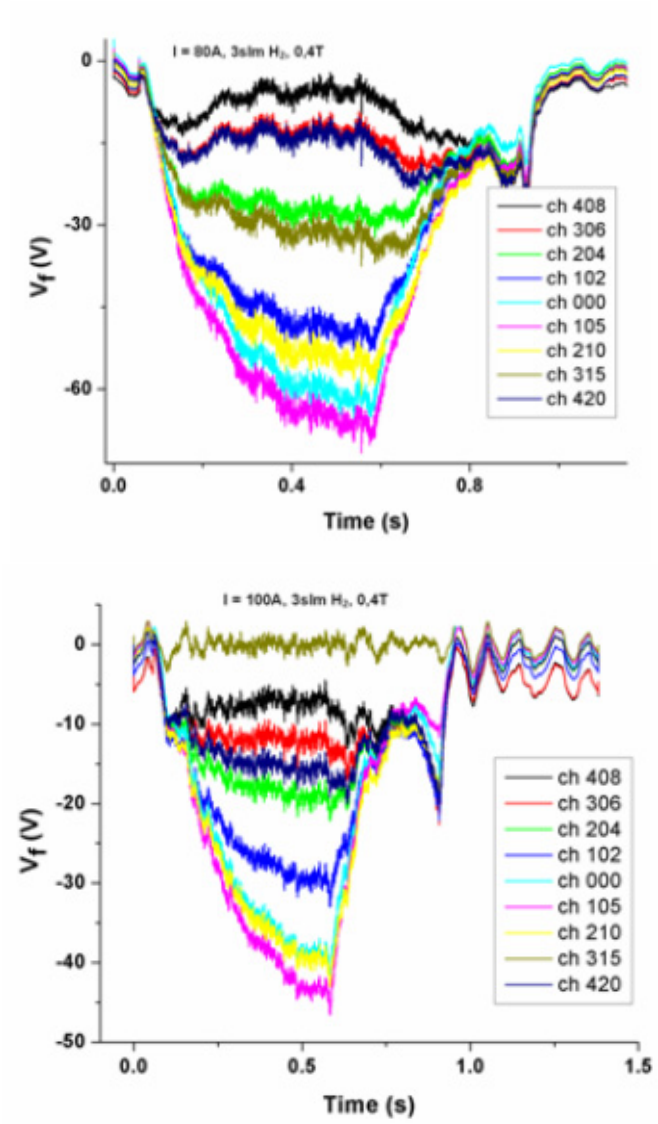

Figure 10: Floating potential variation during plasma pulse for I_d = 80 and 100 A (B = 0.4 T)

By increasing the discharge current from 80 to 100 A the floating potential in front of target decreases as a consequence of the plasma density increase and the decrease of electron temperature. The time variation of the floating potential provides information of the plasma source operation. Figure 11 shows the influence of the source Cu sputtering on the floating voltages measured on the collector.

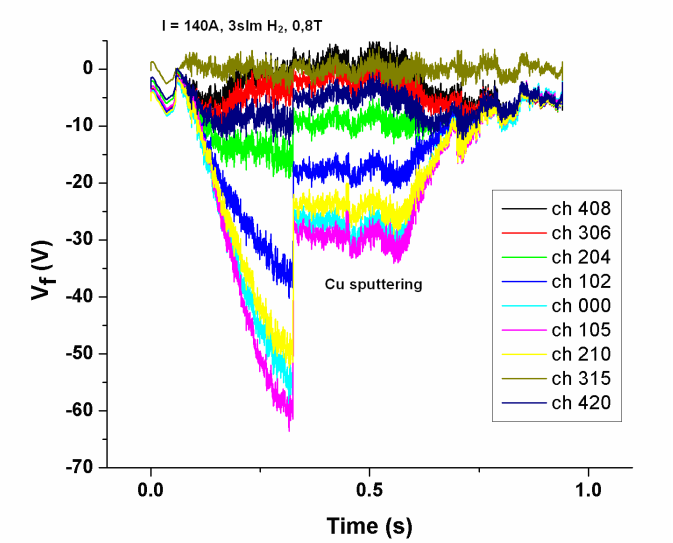

Figure 11: The influence of Cu sputtering on floating voltages

An experiment was imagined to register the currents flowing between different collectors of the analyzer. A Tektronix inductive DC current calibrated probe was used for that. Two collectors were connected together and the rest of the collectors were grounded by 0.2 Ω resistors. Some results are presented in Figure 12. Small currents have between detected between collectors, of the order of mA, currents determined by different local floating potentials in front of the collectors. These currents are much smaller than the currents flowing through the grounded electrodes. Nevertheless, the results show that when a metallic surface is in contact with plasma having a non uniform distribution of the floating potential, currents may appear along the metallic surface. More experiments are necessary in order to understand if the net current flowing into the target affects the plasma-surface interaction.

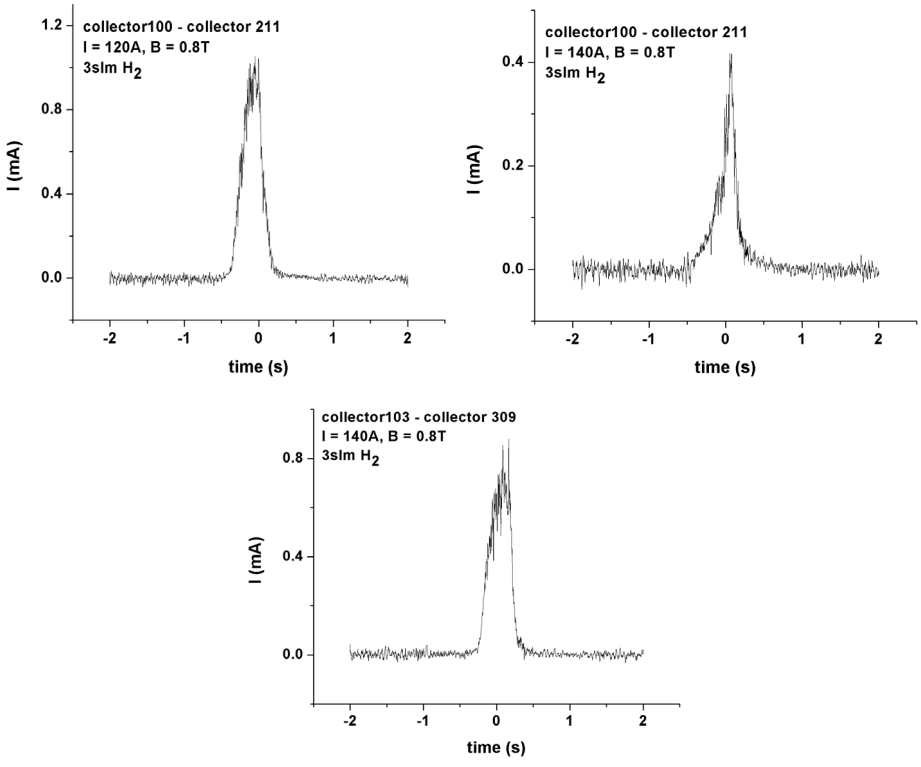

Figure 12: Currents flowing between two collectors during plasma pulse

3. Development of numerical codes for the simulation of magnetised plasma devices (application to Pilot-PSI)

6.3.1. Development of a 2D fluid model

The two fluid models (2D in argon) previously developed, one for the neutrals flow and the other for the charged particles (electrons and positive ions) were coupled for a complex and realistic description of the plasma produced in Pilot-PSI. Preliminary results were obtained for the radial and axial distributions of plasma parameters, such as plasma potential, charged particle densities and fluxes. However, further investigations have to be done on the stability of the numerical code. In this version, oscillations of the plasma parameters develop at the target surface and propagate into the discharge.

3.2. Development of a 2D PIC-MCC model

Milestone 1: *Monte Carlo Collisions module*

A module for particles collisions has been developed using Mote Carlo Method. Several activities were performed to achieve this specific objective:

- bibliographic studies for different cross-sections taking into account for elementary processes for plasma (Ar and/or H/H_2): elastic scattering of electrons, ionization, global excitation and resonant charge exchange for ions [5];
- all the cross-sections for the above processes are read in our module from different data files, making thus possible to be very flexible if intending to change plasma species used in the simulation [6];
- a random number generator was developed for Monte Carlo method inspired from GNU Scientific Library (GSL) [7];
- Monte Carlo Collision (MCC) module programming and testing.

Milestone 2: *Code parallelisation*

As it was previously mentioned, our 2D PIC-MCC simulation code is indented to be accelerated by means of parallel code machine:

- Message Passing Interface standard MPICH2 library have been installed and used in main program function;
- Porting this Code on Scientific Linux installed on our machine (2 CPUs dual core) and on a computing grid from our organization (UAIC): **High Performance Computing** - Cluster of 520 computing cores (approx. 4 TFlops) [8].

Milestone 3: *PLUAIC – alpha release (version December 2009)*

All the modules previously developed plus the module for solving the equation of motion of the charged particles were linked together into a test program PLUAIC (alpha release). This release has some limitation due to the testing and bug elimination processes:

1. the total number of charged particle species is 2, electrons and positive ions (Ar^+ or H^+);
2. maximum of total simulation particles in the program is limited to 100.000;
3. evaluation of the electrical potential into a arbitrary spatial point (r,θ,z) is done using the first approximation relative to the spatial mesh;
4. no external electrical circuit is considered in this version;
5. the parallelisation of the code is rewritten using multithreading technique for a rapid and optimization test (PLUAIC program running into 1, 2, 4, 8 threads on a 2 dual-core CPUs machine and on 8 dual-core CPUs machine).

Table 1: Remarks on code's modules

Module	Issue	Observations
Equation of motion	- leap-frog method	- good results if there is a good time step and mesh spatial grid values. TO DO: use different methods for electrons and ions motion solvers.
Field solving equations	- FFT 2D method for Poisson equation - electrical charge density evaluation	- very fast comparing to direct solver method; - first approximation is used: all the electrical charges from a spatial cell are uniformly distributed to the first neighbour cells. TO DO: interpolation for electrical charge density evaluation.
Mote Carlo Collisions	- random generator - real cross sections for elementary processes	- method inspired from GNU Scientific Library (GSL); - elastic scattering of electrons, ionization, global excitation and resonant charge exchange for ions. TO DO: why there are less elementary processes involved in simulations than expected?
Code parallelisation	- MPI library - multithreading technique	- standard MPICH2 library has been installed and used in the main program function; - for the first release of the program only multithreading technique was used because of the waste of resources in a computing ring. TO DO: eliminate the limitations for the number of species and the total number of particles.
External circuit	- not yet implemented	TO DO: to be implemented.

References

[1] J. Brotankova, J. Adamek, *et al*, *Czech. J. Phys.*, Vol. **56**, No. 12, 1321-1327 (2006)
[2] G. J. van Rooij, V. P. Veremiyenko, *et al*, *Appl. Phys. Lett.* **90**, 121501 (2007)
[3] H. J. van der Meiden, R. S. Al, *et al*, *Rev. Sci. Instrum*. **79,** 013505 (2008)
[4] P.C. Stangeby, "The Interpretation of Plasma Probes for Fusion Experiments", Chapter 5 in *Plasma Diagnostics Volume 2, Surface Analysis and Interactions*, Ed O. Auciello and D.L. Flamm (Boston: Academic) 157-209 (1989)
[5] D. Tskhakaya and S. Kuhn, *Contrib. Plasma Phys*. **42** (2–4), 302–308 (2002)
[6] XOOPIC plasma simulation http://ptsg.eecs.berkeley.edu/pub/codes/xoopic/
[7] GNU Scientific Library (GSL) (http://www.gnu.org/software/gsl/)
[8] High Performance Computing facilities http://stoner.phys.uaic.ro/amon/facilities.html